This article has been accepted for publication in IEEE Transactions on Electron Devices. This is the author's version which has not been fully edited and content may change prior to final publication. Citation information: DOI 10.1109/TED.2023.3301841

The Regime of the Efficiency Increase by Use of Long Circuits in the THz Cherenkov Oscillator

E. Khutoryan, A. Kuleshov, S. Ponomarenko, K. Lukin, Y. Tatematsu, M. Tani

***Abstract* — The self-consistent problem of EM field excitation by a rectilinear electron beam moving along either uniform grating (Smith-Purcell radiation) or bi-periodic grating (leaky wave radiation of spoof surface plasmon polariton) and the influence of the excited EM field on the electron beam has been considered. It is shown that a deceleration of electrons (energy transfer from electrons to EM wave) in both the Smith-Purcell radiation and the leaky wave radiation of the spoof surface plasmon polariton regimes may occur for essentially increased slow-wave circuit length in comparison with conventional BWO and orotrons. This allows either to enhance the output power or to reduce the beam current density of the THz oscillator. The simulations show the output power of 18 W with the corresponding efficiency of 1.5 % at 0.64 THz in the case of the circuit length of 28 mm while the current density is 180 A/cm^2. Such operation is based on the hybrid bulk-surface mode excitation in the THz oscillator cavity with bi-periodic grating and the top reflector for leaky waves. This is promising for the increase of the output efficiency higher than 1% and providing the Watt level of output power in the THz oscillator based on hybrid bulk-surface modes.**

***Index Terms*— THz radiation, Smith-Purcell radiation, leaky wave, spoof surface plasmon polariton, hybrid bulk-surface mode, Cherenkov VED, bi-periodic grating, sheet electron beam.**

I. Introduction

THE activity to fill the THz gap by the use of vacuum electron devices (VEDs) which are efficient in the microwave range is going in many laboratories all over the world [1]. Cherenkov VEDs are good candidates for compact-size devices to generate the EM radiation up to 1.5 THz [2]-[9] for various THz applications [10]-[12]. However, such effects as confinement of RF field near slow wave circuit, high-frequency ohmic losses, technological limits, a decrease of efficiency of output waveguides etc. cause quite high starting currents and low output power levels of the THz non-relativistic compact Cherenkov devices [1]-[9], [13], [14]. As can be seen from the Table I, the Watt level of the output power (required for the DNP-NMR spectroscopy [12]) at the frequencies higher than 0.25 THz among compact Cherenkov oscillators is achievable only in EIO [7] (with the output efficiency less than 1%), though it is most expensive oscillator with narrow frequency tuning range. For the frequencies higher than 0.5 THz, the Watt level of the output power and efficiency of 1% is significant challenge for the compact VEDs and achieving of this goal is very important for such applications as DNP-NMR spectroscopy and other ones requiring Watt level of the output power.

It is well known that in microwave VEDs the starting current can be easily reduced by the increase of the interaction length [13] and operating-to-starting current ratio can be quite high. Due to ohmic loss causing high attenuation γ of the surface wave along a grating ($E \sim e^{-\gamma z}$) in the THz range, the length increases more than $L_{max} \approx 1/\gamma$ has low effect on the starting current in conventional surface wave THz BWOs. In the bulk (volume) wave VEDs such as DRO and Orotron the grating length increase is usually accompanied with complications in the special multi-focusing upper mirror of the open resonator [15], [16]. The hybrid bulk-surface wave oscillator has no such

TABLE I
PARAMETERS OF MODERN CHERENKOV VEDS

VED	Frequency range, GHz	Beam voltage/ current	Maximal CW output power, W	Maximal Efficiency, %
Clinotron [9]	220-270	4 kV /120 mA	0.3	0.06
EIO [7]	260-267	12 kV /150 mA	15	0.8
Orotron [16]	300-340	8 kV /120 mA	0.3 (pulsed)	0.03
Clinotron [6]	350-410	4 kV /120 mA	0.05	0.01
BWO OV-32 [2]	370-535	3 kV /60 mA	0.005	0.003
BWO OV-80 [2]	526-714	3 kV /60 mA	0.005	0.002
EIK [8] (under design)	668-678	25 kV /100 mA	8 W (predicted)	0.32

This paragraph of the first footnote will contain the date on which you submitted your paper for review.

E. Khutoryan, A. Kuleshov, K. Lukin are with the O. Ya. Usikov Institute for Radio Physics and Electronics, National Academy of Sciences of Ukraine, Kharkiv, 61085 Ukraine (e-mail: edkhut@gmail.com; jeanalexkh@gmail.com; lukin.konstantin@gmail.com).

S. Ponomarenko is with the Max-Plank Institute for Plasma Physics in Greifswald, Germany (e-mail: sergyponomarenko@gmail.com).

K. Lukin is also with the Faculty of Electrical and Computer Engineering, University of Campinas, UniCamp, Brazil (lukin.konstantin@gmail.com).

Y. Tatematsu and M. Tani are with the Research Center for Development of Far-Infrared Region, University of Fukui, Fukui, 910-8507 Japan (e-mail: tatema@fir.u-fukui.ac.jp; tani@fir.u-fukui.ac.jp)

This article has been accepted for publication in IEEE Transactions on Electron Devices. This is the author's version which has not been fully edited and content may change prior to final publication. Citation information: DOI 10.1109/TED.2023.3301841

restrictions and the starting current can be essentially reduced [17]-[19] provided the beam transportation problem being solved. However, at moderate electron beam current, the theory of conventional VEDs [13], [14] says that the long interaction space results in such effects like electron beam overbunching, radiation output efficiency decrease, decrease of resonant properties (due to wave attenuation), etc. that causes the output power limitation and the excitation of multifrequency and stochastic/chaotic oscillations [20], [21]. Therefore, there is a tradeoff between low starting current and high output power that limits the length of the interaction space.

In this paper we show that due to peculiarities of the Smith-Purcell radiation (SPR) [15], [22]-[25] and those of the leaky wave spoof surface plasmon polariton (LW SSPP) [17]-[19], [26]-[28] the effective beam-wave interaction with no automodulation regime can be provided for long gratings even in the deep non-linear regime with electron beam overbunching. The same time, in this paper we show that the electron and output efficiencies aren't saturated with the interaction length increase even at high beam current that is quite different from the conventional Cherenkov VEDs features [14]. This property of the hybrid bulk-surface mode allows either the efficiency increase at high beam current density or keeping the same efficiency at the reduced beam current density by using longer circuits. This is promising for the increase of the output power of a single frequency mode in the THz oscillators based on both he SPR and the Hybrid Bulk Surface Modes (HBSM) [17], [18].

The presented 2D geometry is justified by the good agreement between 2D and 3D consideration for HBSM [18]. In the 3D configuration, it is assumed to apply the sheet electron beam of 2 mm width with lower current density in comparison with pencil-like beam, which was already utilized for the surface wave 0.4 THz clinotron [6].

II. Self-Consistent Set of The Problem

Let's consider the rectilinear electron beam at $y=a$ with initial velocity $v_0 = \beta c$ (β <1) which is modulated in the gap at the start of the grating and further moving above the grating over the distance L_g in an infinite magnetic focusing field (Fig. 1). The self-consistent 2D problem involves description of both the excitation of EM fields and their interaction with the electron beam.

Therefore, for the rigorous self-consistent analysis we should solve the problem of the diffraction of the EM wave associated

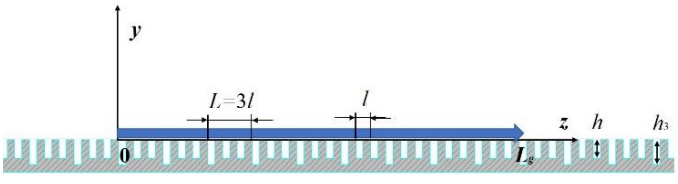

Fig. 1. Theoretical model of the finite rectilinear electron beam flowing along infinite bi-periodic grating

with the finite RF current in the free space ($I(z) = A(z)e^{ih_e z - i\omega t}$, 0<z<$L_g$), on the grating and to substitute

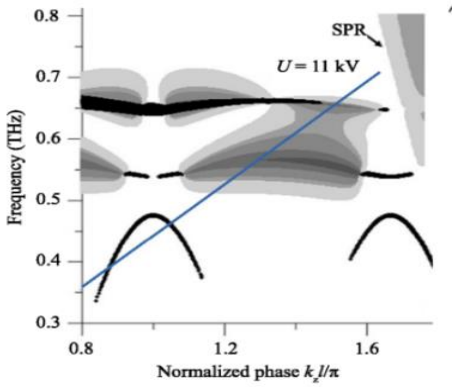

Fig. 2. The 3D map of the absolute value of $W(k)$ which is solution of the diffraction problem for the infinite current wave. The grating period l=70μm, the regular groove depth h=90 μm, the depth of every 3rd groove h_3=120 μm.

the obtained electric field z-component in the beam area $E_d(I)$ into the electron motion equation.

The decomposition technique [29] was modified in [26] to solve the diffraction problem for bi-periodic grating for the infinite current wave $A(k)e^{ikz-i\omega t}$. To find the EM field excited by the nonlinear current of finite-length electron beam, the FT is used [17], [24]:

$$A(z) = \int_{-\infty}^{\infty} A(k_z)e^{ik_z z}dk_z\ ,\ A(k_z) = \frac{1}{2\pi}\int_0^{L_g} A(z)e^{-ik_z z}dz$$
$$E_d = e^{ih_e z}\int_{-\infty}^{\infty} A(k_z)e^{ik_z z}\sum_n W(h_e + k_z + \frac{2\pi n}{L})e^{i\frac{2\pi n}{L}z}e^{\sqrt{k^2-\left(h_e+k_z+\frac{2\pi n}{L}\right)^2}\,a}dk_z \quad (1)$$

where $W(k)$ is the solution for the infinite-length current wave found in [27], [28], [30]. The map of $W(k, f)$ is shown in Fig. 2 for the bi-periodic 3-stage grating (every 3rd groove is of modified groove depth $h_3 \neq h_1$) l = 0.07 mm, h_1 = 0.09 mm, h_3/h_1 =1.3.

Poles of $W(k)$ correspond to eigenmodes and without losses (ohmic/dielectric or leaky wave radiation) the poles have only real part. Eigenmodes of bi-periodic grating are either pure surface waves (pure SSPP) or surface waves with leaky wave radiation (LW SSPP) which are the basis of the SSPP leaky wave antennas (SSPP LWA) [28]. From the Fig. 2 one can see that due to the additional loss for outgoing radiation, $W(k)$ is less resonant for LW SSPP (the higher the loss, the smoother $W(k)$) than that of the pure SSPP. In contrast to eigenmodes, the SPR is not an eigenmode of an open grating and, therefore, $W(k)$ is quite smooth in this region as follows from the SPR theory [24], [25]. In the case of the top conductive wall the situation becomes opposite: narrowest $W(k)$ is for the SPR which in resonance with bulk modes of the closed waveguide [15], [24], and $W(k)$ in the region of pure SSPP is almost the same as for open grating and is the widest [17].

III. Loss Of Electron Energy At The SPR Excitation

Let's consider the simplest case of the SPR excitation in the linear regime, for which motion equation may be transformed

This article has been accepted for publication in IEEE Transactions on Electron Devices. This is the author's version which has not been fully edited and content may change prior to final publication. Citation information: DOI 10.1109/TED.2023.3301841

into [15]:

$$\frac{\partial^2 I}{\partial z^2} - 2ih_e \frac{\partial I}{\partial z} - h_e^2 I = CE_d(I) \qquad (2)$$
$$I_z(z=0) = 0;\ I_z'(z=0) = I_0'$$

The second boundary conditions appear due to the velocity modulation. Due to the abovementioned fact of low resonant SPR condition and the linear approximation, $W(k)$ can be expanded as:

$$W(h_e + k_z) \approx W(h_e) + \sum_{m=1}^{m_0 << N} (k_z)^m \frac{W^{(m)}(h_e)}{m!} \qquad (3)$$

And the synchronous electric field may be represented as

$$E_d = e^{ih_e z} W(h_e) \int_{-\infty}^{\infty} A(k_z) e^{ik_z z} dk_z + $$
$$+ e^{ih_e z} \sum_n \frac{W^{(n)}(h_e)}{n!} \int_{-\infty}^{\infty} A(k_z)(k_z)^n e^{ik_z z} dk_z$$

From where we can write:

$$E_d = W_0 I + \sum_{m=1}^{m_0 << N} (i)^m \frac{W^{(m)}}{m!} \frac{d^m I}{dz^m}$$

Since $W(k)$ is smooth and we consider the linear regime, derivatives in the sum (3) can be omitted and the final equation is:

$$\frac{\partial^2 I}{\partial z^2} - 2ih_e \frac{\partial I}{\partial z} - h_e^2 I = CW_0 I$$

which solution is:

$$I = \frac{I_0'}{2ih_q}\left(e^{ih_q z} - e^{-ih_q z}\right)e^{ih_e z} \qquad (4)$$

where $h_q = \sqrt{-CW_0} = \frac{\omega_q}{v_0}$.

Due to the properties of W_0 for the SPR [29], the slow space charge wave grows along z, while the fast space charge wave decays [30], [31] causing the self-amplified spontaneous emission (SASE) [31]. As a result, the lobe in the radiation pattern corresponding to the slow space charge wave is more intensive (Fig. 3(a)) and the average electron velocity decreases with z (Fig. 3(b)).

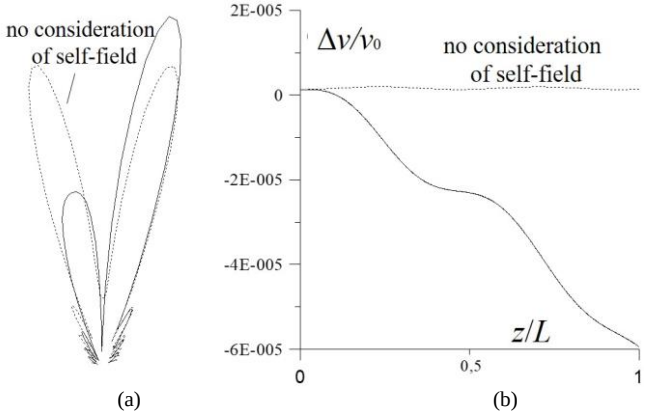

(a) (b)

Fig. 3. Radiation pattern of the SPR (a) and the average electron velocity decrease along the axis z (b).

IV. Excitation Of The Leaky Wave SSPP

In the case of eigenmodes excitation when $k=k_{SSPP}$, the absolute value of $W(k_{SSPP})$ is greater than that of $W(k_{SPR})$ at the excitation of the SPR which is not an eigenmode. Therefore, the linear approximation is valid for much lower beam currents for the LW SSPP rather than for the SPR case. One more distinction from the previous section in the solving of Eq. (1) is that the expansion in series as in (3) is no more valid due to $W(k)$'s poles at $k=k_{SSPP}$.

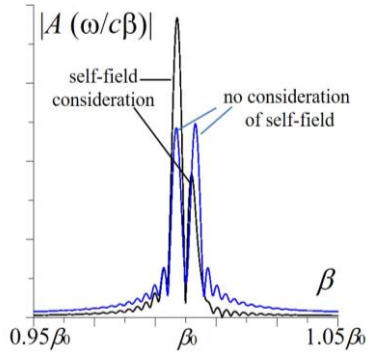

Fig. 4. Spectral distribution of the RF current at excitation of the LW SSPP in the linear regime. Beam voltage U=17800 V, beam current J=6 mA/mm, f=0.66 THz.

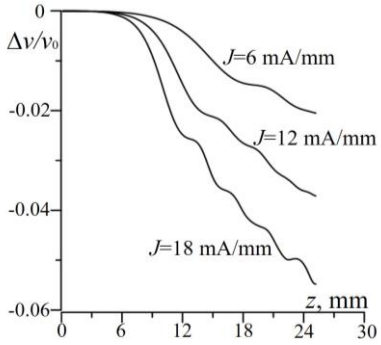

Fig. 5. Average electron velocity dependence on the axial coordinate at the case of the LW SSPP excitation at several beam currents. U=17800 V.

Therefore, the self-consistent solution in the case of the LW SSPP excitation by the modulated electron beam has been carried out numerically using iteration procedure: first we have solved the nonlinear electron motion equation using macro-particles approach [32] to find the first harmonic of the RF current $I(z)$ and it's Fourier components $A(k)$. On the second step we have found the electric field in the beam area E_d using (1). Substituting the found E_d into the motion equation we again have found the RF current $I(z)$ and so on. The iteration procedure was stopped after good accuracy was achieved. The number of iterations increased in the non-linear regime and it is strongly dependent on the beam current, electron transit length L_g, electrons velocity v_0 and dependence $W(k)$ in the vicinity of h_e. Let's notice that in contrast to the so called "self-consistent

This article has been accepted for publication in IEEE Transactions on Electron Devices. This is the author's version which has not been fully edited and content may change prior to final publication. Citation information: DOI 10.1109/TED.2023.3301841

theory" used for conventional VEDs, where "cold modes" interact with an electron beam, here we obtain solution without this approximation.

First, let's consider the low current case to study the linear regime. Numerical solution of (1) shown in the Fig. 4 provides increased spatial Fourier component $A(k)$ of the RF current corresponding to the slow space charge wave that is similar to the SPR case. The average electron velocity monotonously decreases along grating as in the SPR case and with an increase of the beam current this effect becomes more prominent. The most distinguishing from the conventional surface wave regime is that there is almost no saturation with length even when electron efficiency approaches 10% (roughly $\eta \approx -2\Delta v/v_0$ corresponding to the curve where $\Delta v/v_0 \approx -0.05$ at the end of the interaction space,) as can be seen in Fig. 5.

The electrons velocity decrease results in the widening of the RF current spatial spectra $A(k)$ and in appearing of components

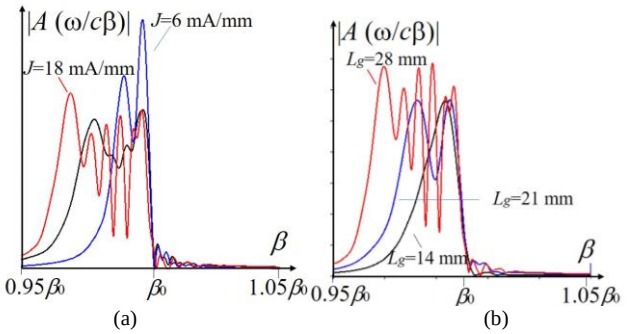

Fig. 6. Spatial FT of the RF current spatial spectral $A(k)$ in the non-linear case of the LW SSPP. a) at various beam currents; b) at various lengths.

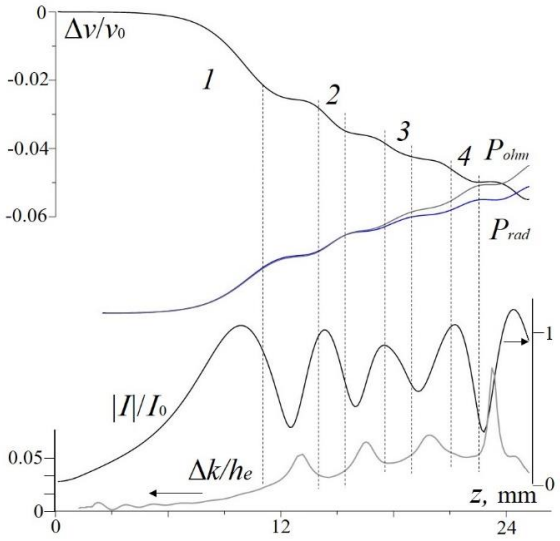

Fig. 7. Axial dependence of the average electron velocity, normalized power of leaky radiation and ohmic loss P_{rad} and P_{ohm}, absolute value of the RF current $|I|$ and wavenumber Δk. Beam voltage U=17800 V, beam current J=18 mA/mm, f=0.66 THz.

with larger wavenumber k (or lower phase velocity v_{ph} since $k=\omega/v_{ph}$) as shown in Fig. 6. This becomes more prominent with the increase of either the beam current (Fig. 6(a)) or the interaction length (Fig. 6(b)).

From the Fig. 6(b) one can see that with the length increase, additional wavenumbers appear at the spatial spectra $A(k)$ while the waveform $A(k)$ appeared at smaller lengths remains almost unchanged. To find out the reason of such dependencies of the velocity and spatial spectrum on z, we have studied in detail the amplitude and phase of the RF current and RF field along the grating.

First, we separate absolute value and phase of the RF field to find the "instant" wavenumber $\Delta k(z)$:

$$E_d(z) = |E(z)| e^{i\varphi(z)} e^{ih_e z} \qquad (5)$$
$$\varphi(z) = \int_0^z \Delta k(\tilde{z})\, d\tilde{z}$$

Fig. 7 demonstrates the axial dependence of the electron average velocity $\bar{v}(z)/v_0 - 1$ together with the normalized power of the leaky radiation P_{rad} and ohmic loss P_{ohm}, the absolute value of the RF current first harmonic $|I|$ and the wavenumber shift Δk.

The areas 1-4 marked on the Fig. 7 correspond to the strong velocity decrease, while between these areas the velocity derivative is almost zero. Almost the same behavior is of P_{rad}. The behavior of Δk is opposite: at areas 1-4 it slightly varies, while between the areas the phase is rapidly switched [33]. Areas of the phase switch practically coincide with RF current minima, i.e., near electrons debunching regions. Therefore, areas $\Delta k \approx const$ cause the coherent leaky radiation with increased intensity, whereas between these regions the radiation is not coherent and its intensity is low. In its turn, the power of ohmic (dielectric) loss depends only on the RF field absolute value and therefore, its growth is not strong when absolute value of RF field is low. These areas usually coincide with the areas of the abrupt phase shift, and because of this the behavior of P_{rad} and P_{ohm} is similar. Thus, comparing Fig. 6(b) and Fig. 7 we conclude that practically monotonous widening of the $A(k)$ with length is caused by the coherent leaky wave radiation and the average velocity decrease occurs in these areas due to leaky wave radiation loss.

In the linear regime the leaky wave radiation angle can be roughly found from the LW SSPP dispersion as:

The H_x RF pattern obtained at the linear case shown in Fig. 8(a) agrees with (6) very well. However, in the nonlinear regime when $\Delta k \neq const$, Eq. (6) can be used for rough angle estimation only for areas 1-4 where $\Delta k \approx const$. From (6) we can also roughly find the angle change with the average velocity as $\Delta\alpha \approx \dfrac{\Delta\beta_e}{\beta_e^2 \sin\alpha}$, that for the parameters of the grating and beam voltage corresponding to the Fig. 7 results in $\Delta\alpha \approx -10°$ for $\Delta\beta_e = -0.05\beta_e$.

$$\cos\alpha = \frac{k_z}{k} = \frac{h_e\left(1+\omega_p/\omega\right) - \dfrac{4\pi}{3l}}{k} = \frac{1+\omega_p/\omega}{\beta_e} - \frac{2}{3}\frac{\lambda}{l} \qquad (6)$$

The RF field pattern calculated for this case (Fig.8(b)) confirms the assumption that areas with different $\Delta k(z)$

This article has been accepted for publication in IEEE Transactions on Electron Devices. This is the author's version which has not been fully edited and content may change prior to final publication. Citation information: DOI 10.1109/TED.2023.3301841

emit with slightly different radiation angles. The angle of leaky wave radiated from the area 1 coincides with the linear case, while the radiation direction from the last grating segment is changed by the angle which is quite close to our rough estimation.

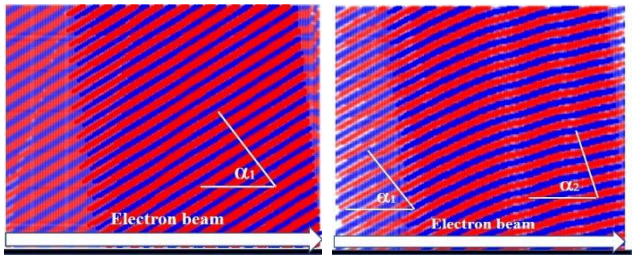

(a) (b)

Fig. 8. The leaky wave radiation pattern in the linear case (J=1 mA/mm) (a) and in the non-linear case (J=18 mA/mm) (b).

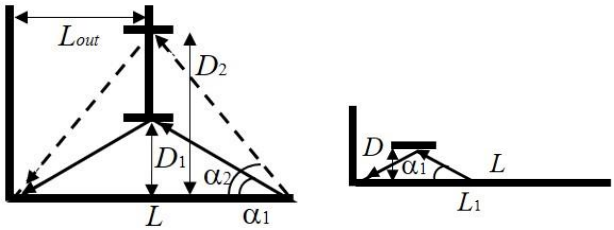

(a) (b)

Fig. 9. Sketches demonstrating rays which correspond to the radiating harmonic for cases of different distances between grating and reflector D (a) and various positions of a reflector (b).

V. Oscillator Based On The HBSM

In the previous section it was assumed that an electron beam was modulated at $z\cong0$. To provide the regime of self-excitation, a conducting wall can be placed above a grating for the reflection of the leaky wave back to a grating at the area $z\cong0$ (Fig. 9) to modulate an electron beam. In such way we create the feedback for the oscillatory mode. In the configuration with a reflector or a conducting wall, the reflected leaky wave transforms into the bulk mode of the waveguide, which together with the SSPP constitute the hybrid bulk-surface mode (HBSM) [17], [18], [26].

The regime with a single reflection considered in [18] is lesser sensitive to ohmic loss and, hence, the starting current can be substantially reduced by the grating length increase (Let's notice that an increase of the length of the interaction space also requires detailed electron beam transportation analysis, which is omitted here).

From Fig. 9(a) one can see that the grating length, the distance to reflector and the radiation angle are roughly related as

$$L_g \tan\alpha \approx 2D \qquad (7)$$

As it was shown in the previous section, such regime doesn't much suffer from a beam overbunch and, hence, we may assume that the efficiency should grow with length with no saturation. To verify this assumption together with the theoretical results of the Section IV, in this section we carry out the PIC FDTD simulations using MAGIC2D [34]. To properly consider the effect of ohmic loss in simulations, we set the value of material conductivity as 1.7×10^7 S/m that is about 3 times lower than that of the perfect oxygen-free copper (usually such value in 0.5-0.7 THz range is supposed to be due to surface roughness, etc.). The 3-stage grating parameters and the beam voltage are as in the previous section: l = 0.07 mm, h_1 = 0.09 mm $h_3 = 1.3h_1$, U=17800 V. Beam emitter thickness is 0.02 mm. At L_g=28 mm and D=17 mm (that approximately satisfies (7)) the 2D starting current was about I_{st} = 6 mA/mm (in the 3D case it is equivalent to J=30 A/cm^2). The radiation angle agreed very well with the condition (7) and was the same for whole grating. To study the strongly nonlinear regime, we took $I=6I_{st}$ and have simulated two configurations shown in Fig. 9(a) and Fig. 9(b). The results of the first simulation of the nonlinear regime using the same grating-reflector distance as in the linear regime (D=17 mm), have shown that due to the change of the radiation angle in the nonlinear regime, the Eq. (7) doesn't hold. This results not only in not optimal feedback length, but also in the not optimal width of the radiation output. Moreover, because of high leaky wave intensity, the feedback becomes too deep that can lead to the oscillation automodulation [20, 21]. Therefore, the distance D should be changed to keep the optimal condition in the non-linear regime (according to our simulations it can be also attained by the upper reflector inclination). According to rough estimations made in the previous section, the new value of distance was taken as D=20 mm. However, no self-excitation occurred

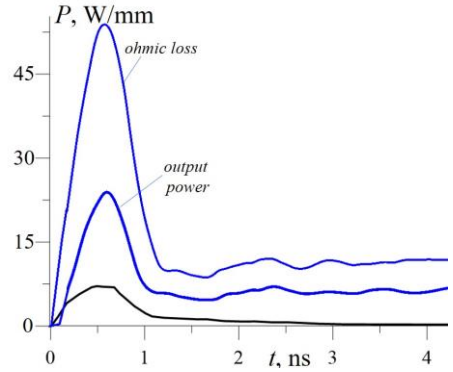

Fig. 10. The power of ohmic loss in the "soft" regime (black) and the power of ohmic loss and the output power vs. time in the hard regime (blue curves) at D=20 mm.

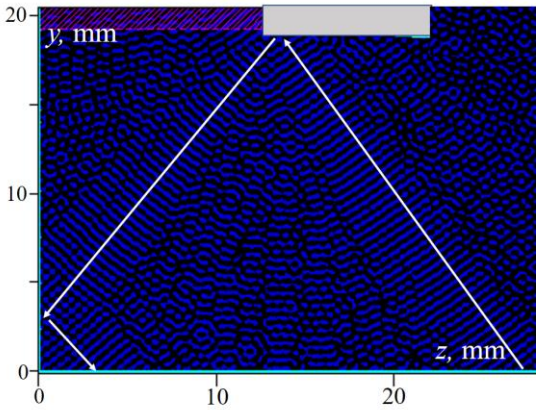

Fig. 11. RF field patterns during transient in the case of low excitation signal at D=20 mm.

This article has been accepted for publication in IEEE Transactions on Electron Devices. This is the author's version which has not been fully edited and content may change prior to final publication. Citation information: DOI 10.1109/TED.2023.3301841

(black curve in Fig. 10) and the RF field pattern after 1 ns is shown in Fig. 11. This made obvious that since the RF field amplitude is small during transient, the feedback condition (7) should hold for the "linear" α at the soft excitation. In the case of *D*=20 mm, the reflected wave doesn't fall onto the grating and, therefore, there is no feedback.

To check if the oscillation can be hard-excited, we have strongly increased the initial signal using initial bunched beam with the higher current:

$$I=\begin{cases}12I_{st}, i<ft<i+0.5\\ 0, i+0.5\le ft\le i+1; i=0,1,2..,\mathrm{int}(f0.7\ ns)\\ 6I_{st},\ t>0.7\ ns\end{cases} \quad (8)$$

In the case of the driving signal according to (8), the power dependence on time is shown in Fig. 10 where one can see that the steady state was attained after about 5 ns. The oscillation is excited at the 639GHz with total 2D beam-wave interaction power about 22 W/mm (about 13 W/mm of ohmic loss and 9 W/mm of output power). With the beam voltage and current of 17.8 kV and 36 mA/mm it corresponds to the electron efficiency is about 3.5 % and the output efficiency was about 1.5% that is in good agreement with the phase space shown together with the RF field pattern in the Fig. 12.

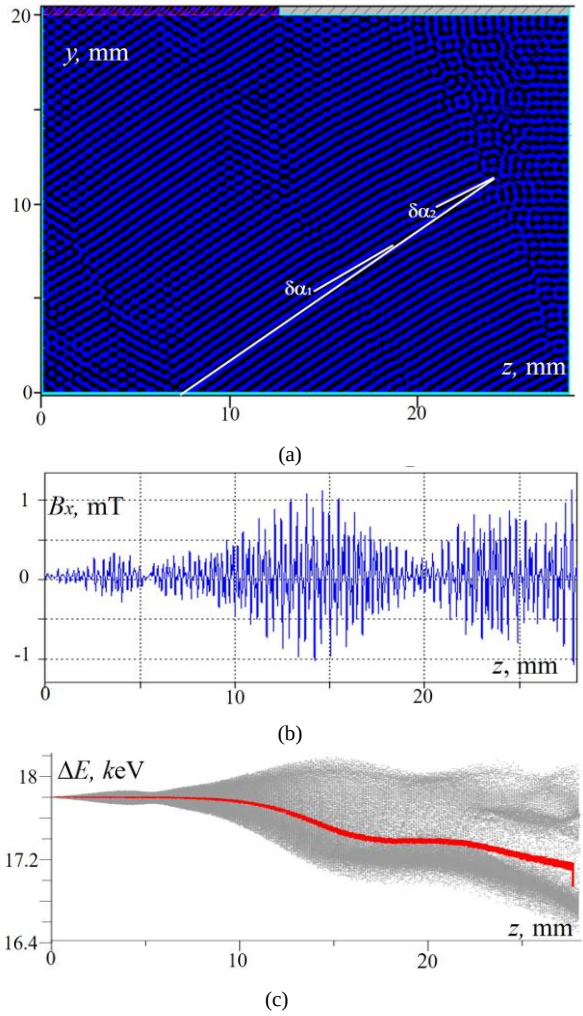

Fig. 12. Steady state RF *Bx* field patterns (2D (a) and 1D (b)) and electrons energy versus axial distance (c) in the case of hard excitation at *D*=20 mm.

As it was shown in [18], in the case of the 3D configuration we can roughly estimate the output power as the 2D value multiplied by the electron beam width and for the 2 mm wide electron beam (typical for THz clinotrons fabricated in IRE NAS of Ukraine [6], [9], [13]) the output power is about 18 W. One can see that the radiation angle changes along the grating as theoretically predicted. Also, there are two areas of monotonous average velocity decrease where the RF field phase is almost constant separated by debunch area, where the RF filed phase is abruptly changes. The hard excitation regime due to the radiation angle change points out to the hysteresis on the waveguide height. This in its turn additionally allows to control the mode competition at high beam current. Another way to place a reflector is as shown in Fig. 9(b) since at the high beam current, the starting grating length can be shortened together with *D* as follows from Eq. (7). The results of the such configuration simulation are shown in the Fig. 13- 15. The output power for this configuration is the total power propagating through the top boundary. To provide the beam voltage sweep shown in the Fig. 13, the voltage was increased by $\triangle U$ = 100 V every 5 ns during the simulation.

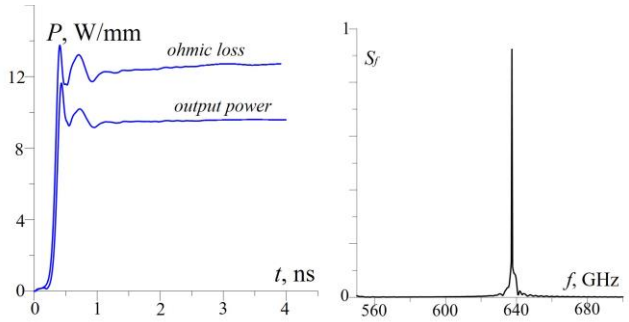

Fig.13. The result of the simulations for configuration shown in Fig. 9 (b) at *U*=17.8 kV, *I*=36 mA/mm, *D*=3.2 mm. (a) the power of ohmic loss and the output power vs. time; (b) the normalized spectrum of the output signal.

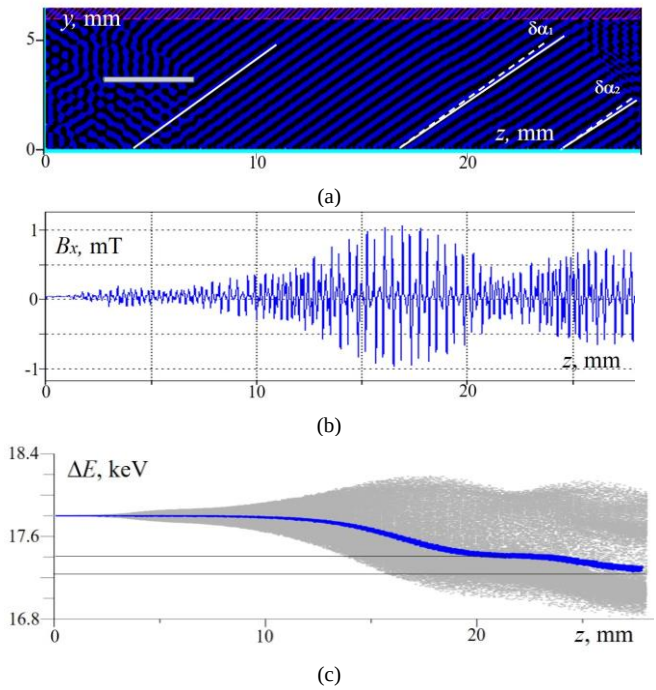

Fig.14. Steady state RF field patterns (2D (a) and 1D (b)) and electrons energy versus axial distance (c) for the configuration shown in Fig. 9 (b).

This article has been accepted for publication in IEEE Transactions on Electron Devices. This is the author's version which has not been fully edited and content may change prior to final publication. Citation information: DOI 10.1109/TED.2023.3301841

Fig. 14 demonstrates that after soft self-excitation at the first grating segment, the excited LW SSPP at the second grating segment causes almost monotonous velocity decrease and serves as the output radiation. The power and frequency dependencies on the beam voltage shown in Fig. 15 when the distance between grating and reflector D=3.2 mm indicate the electron frequency tuning range about 10 GHz. Simulations show that combined mechanical (change D) and electron frequency tuning is about 15 GHz.

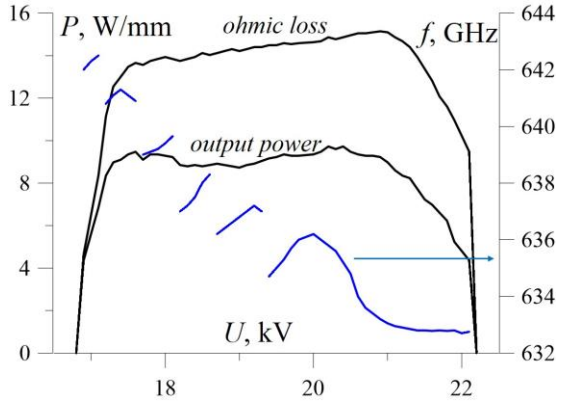

Fig.15. Frequency and the power of ohmic loss and of output radiation versus beam voltage for the configuration shown in Fig. 9 (b) at I=36 mA/mm, D=3.2 mm.

VI. Experimental Prototype and Research Plan

The experiments described in [26] have demonstrated the excitation of the HBSM in 0.1-0.14 THz range. To confirm the obtained theoretical results, we are planning to carry out the experimental research at the higher frequencies. In this section we briefly describe the design of the experimental prototype and the plan of the future research. The intended experimental study includes the study of the radiation patterns of both the SPR and the LW SSPP as well as the research of the HBSMs excitation in the auto-oscillatory regime. For this goal we have modified the experimental setup that was designed at IRE NAS of Ukraine for the analysis of the diffraction radiation [15], [35]. The scheme and the photo of the prototype is shown in Fig. 14. According to the design, an electron beam moves along a grating in the vacuum chamber (which will be installed and adjusted at an electromagnet). The emitted radiation (SPR or leaky wave radiation) is to be detected by a radiation receiver movable in both azimuth and elevation angles to plot a radiation pattern and located outside of the chamber. To study various regimes at different frequency ranges, a grating, a reflector and an electron gun are made replaceable.

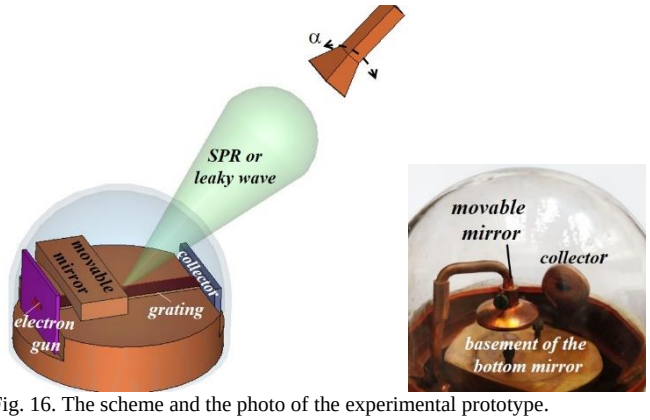

Fig. 16. The scheme and the photo of the experimental prototype.

Following Figures 12 and 14 one can see the correspondence of the theoretical model with the designed prototype for the HBSM excitation in the case of a non-uniform grating installation. Also, such prototype enables study of some other promising regimes for the excitation of the THz radiation:

- in the case of a uniform grating installation, the beam bunching can occur due to the BWO regime while the SPR may occur at the frequency harmonics (SPR FEL) [36]-[40]. When an upper movable mirror is installed the enhancement of this radiation is predicted in [41], [42].
- another possibility of the beam bunching when the upper mirror is installed is the excitation of the DRO oscillation occurring at the first segment of the structure, while along the rest of the structure the bunched electron beam excites the SPR at the same frequency [15]. To distinguish the SPR and the radiation from the open resonator, the 'cold' experiment should precede the "hot" one [35].

VII. Conclusion

The excitation of both the Smith-Purcell radiation and the leaky wave radiation of spoof surface plasmon polariton by rectilinear electron beam moving above the long grating has been studied in the paper. The results of theoretical calculations and FDTD PIC simulations have demonstrated that due to the essential increase of the interaction length, two (contradictory for traditional Cherenkov VEDs) goals may be achieved: the starting current decrease and the output efficiency increase. Specifically, it relates to the THz oscillators based on the hybrid bulk-surface modes due to the higher coupling impedance of LW SSPP than this of the SPR. The carried-out simulations showed more than 10 W of the output power at 0.64 THz in the case of applied sheet electron beam of 2 mm width and beam current density of 180 A/cm^2 that corresponds to the output efficiency of 1.5%. Since the efficiency of the modern compact THz oscillators (as follows from the Table I) is much lower than 1%, the obtained result is very promising for creation of the THz Watt-level Cherenkov oscillators with the output efficiency of several percent. However, we should notice that further study of the sheet electron beam transportation and the output radiation focusing is also required for the achievement of the optimal performances.

References

[1] J. H. Booske et al., "Vacuum electronic high-power terahertz sources," IEEE Trans. THz Sci. Technol., vol. 1, no. 1, pp. 54–75, Sep. 2011.

[2] A. Korolev, S. Zaitsev, I. Golenitskij, Y. Zhary, A. Zakurdayev, M. Lopin, P. Meleshkevich, E. Gelvich, A. Negirev, A. Pobedonostsev, V. Poognin, V. Homich, and A. Kargin, "Traditional and novel vacuum electron devices," *IEEE Trans. Electron Devices*, vol. 48, no. 12, pp. 2929–2937, Dec. 2001, DOI: 10.1109/16.974731

[3] R. Ives, C. Kory, M. Read, J. Neilson, M. Caplan, N. Chubun, S. Schwartzkopf, R. Witherspoon, "Development of backward-wave oscillators for terahertz applications", Proc. SPIE 5070, Terahertz for Military and Security Applications, July 2003, DOI: 10.1117/12.506905

[4] M. Mineo and C. Paoloni, "Corrugated Rectangular Waveguide Tunable Backward Wave Oscillator for Terahertz Applications," in *IEEE Transactions on Electron Devices*, vol. 57, no. 6, pp. 1481-1484, June 2010, DOI: 10.1109/TED.2010.2045678

[5] G. A. Komandin, S. Chuchupa, S. Lebedev, Y. Goncharov, A. Korolev, O. Porodinkov, I. Spektor, A. Volkov., "BWO generators for terahertz dielectric measurements," *IEEE Trans. THz Sci. Technol*., vol. 3, no. 4, pp. 440–444, Jul. 2013, DOI: 10.1109/TTHZ.2013.2255914

[6] S. Ponomarenko, S Kishko, V. Zavertanniy, E. Khutoryan, I. Lopatin, B. Yefimov, A. Kuleshov, "400-GHz continuous-wave clinotron oscillator," *IEEE Trans. Plasma Science*, vol. 41, no. 1, pp. 82-86, Jan. 2013, DOI: 10.1109/TPS.2012.2226247.

[7] A. Roitman, M. Hyttinen, P. Horoyski, E. Sokol, H. Deng, D. Yake, I. Rannachan, P.Mathieson, A. Kingsmill, I. Ifraimov, D. Berry, R. MacHattie, "Development of sub-millimeter high power compact EIKs for DNP and radar applications," *2017 Eighteenth International Vacuum Electronics Conference (IVEC)*, London, UK, pp. 1-2, 2017, DOI: 10.1109/IVEC.2017.8289722.

[8] R. Dobbsa, A. Roitman, P. Horoyski, M. Hyttinen, D. Sweeney, B. Steer, K. Nguyen, E. Wright, D. Chernin, A. Burke, J. Calame, B. Levush, N. Scott Barker, J. Booske, M. Blank, "Design and fabrication of terahertz Extended Interaction Klystrons," *35th International Conference on Infrared, Millimeter, and Terahertz Waves*, Rome, Italy, pp. 1-3, 2010, doi: 10.1109/ICIMW.2010.5613040.

[9] M. V. Mil'cho, I. V. Lopatin, V. V. Zavertanny, A. S. Tishchenko, K. Ilyenko, "CW clinotrons for the short-wave part of the millimeter waveband," *IEEE International Vacuum Electronics Conference*, Monterey, CA, USA, pp. 71-72, 2014, DOI: 10.1109/IVEC.2014.6857495

[10] B. Gompf, M. Gerull, T. Müller, M. Dressel, "THz-micro-spectroscopy with backward-wave oscillators", *Infrared Physics & Technology*, vol. 49, no. 1–2, pp.128-132, 2006, DOI: 10.1016/j.infrared.2006.01.021

[11] A. Dobroiu, M. Yamashita, Y. N. Ohshima, Y. Morita, C. Otani, K. Kawase, "Terahertz imaging system based on a backward-wave oscillator," *Appl. Opt.* vol. 43, no. 30, pp. 5637-5646, 2004, DOI: 10.1364/AO.43.005637

[12] Michaelis V. K., Griffin R. G., Corzilius B., Vega S. (Eds.), *Handbook of high field dynamic nuclear polarization*, John Wiley & Sons, (2019).

[13] G. Ya. Levin, *The Clinotron.*. Kiev, Ukraine: Naukova Dumka Press, 1992.

[14] A. S. Gilmour, Klystrons, traveling wave tubes, magnetrons, crossedfield amplifiers, and gyrotrons. Artech House, 2011.

[15] V. P. Schestopalov, A. A. Vertiy, G. P. Yermak, B. K. Skrynnik, G. I. Khlopov, A. I. Tsvyk, "Difraction Radiation Oscillators", Kyiv: Naukova Dumka 1991.

[16] E. A. Myasin, V. V. Evdokimov, A. Yu. Il'yn, "300 – 350 GHz frequency range orotron with two electron beams", *Journal of Radio Electronics*, no. 7, 2019, DOI: 10.30898/1684-1719.2019.7.7.

[17] E. M. Khutoryan, A. N. Kuleshov, S. S. Ponomarenko, K. A. Lukin, Y. Tatematsu and M. Tani, "Efficient Excitation of Hybrid Modes in a THz Clinotron," *Journal of Infrared, Millimeter, and Terahertz Waves*, vol. 42, no. 6, pp. 671–683, June 2021, DOI: 10.1007/s10762-021-00800-y.

[18] E. M. Khutoryan, A. N. Kuleshov, S. S. Ponomarenko, K. A. Lukin, Y. Tatematsu and M. Tani, "Hybrid Bulk-Surface Modes Excited by a Sheet Electron Beam in THz Cherenkov Oscillator," *IEEE Transactions on Electron Devices*, vol. 69, no. 6 pp. 3407-3412, June 2022, DOI: 10.1109/TED.2022.3168526.

[19] E. M. Khutoryan, A. N. Kuleshov, S. S. Ponomarenko, K. A. Lukin, Y. Tatematsu and M. Tani "THz Cherenkov Oscillator Efficiency Increase by Use of Long Structures", IVEC 2023 — 24th *IEEE International Vacuum Electronics Conference*, Chengdu, China, pp. 472-473, 2023.

[20] S. Kuznetsov, D. Trubetskov, "Haos and hyperhaos in a backward wave oscillator," *Radiphysics and Quantum Electronics*, vol. 47, pp. 341-355, 2004, DOI: 10.1023/B:RAQE.0000046309.49269.af.

[21] V. A. Rakityansky, K. A. Lukin, "Excitation of the Chaotic Oscillations in Millimeter BWO", *Int. J. Infrared and Millimeter waves*, vol.. 6, no. 16, pp. 1037– 1049, 1995, DOI: 10.1007/BF02068275.

[22] S. J. Smith and E. M. Purcell, "Visible Light from Localized Surface Charges Moving across a Grating," *Phys. Rev.*, 92, pp. 1069–1069, November 1953, DOI: 10.1103/PhysRev.92.1069.

[23] B. Bolotovskii, G.Voskresenskii, "Emission from charged particles in periodic structures", *Uspekhi Fizicheskih Nauk*, vol. 94, no. 3, pp. 378-416, January 1968, DOI: 10.3367/UFNr.0094.196803a.0378.

[24] V.P. Shestopalov, *Smith-Purcell Effect*, Nova Publishers, 1998.

[25] P. M. van den Berg and T. H. Tan, "Smith-Purcell radiation from a line charge moving parallel to a reflection grating with rectangular profile," *J. Opt. Soc. Am.* vol. 64, no. 3, pp. 325-328, 1974, DOI: 10.1364/JOSA.64.000325

[26] E. M. Khutoryan, Yu. S. Kovshov, A. S. Likhachev, S. S. Ponomarenko, S. A. Kishko, K. A. Lukin, V. V. Zavertanniy, T. V. Kudinova, S. A. Vlasenko, A. N. Kuleshov, T. Idehara, "Excitation of Hybrid Space-Surface Waves in Clinotrons with Non-uniform Grating," *J Infrared, Millimeter, and THz Waves*, vol.39, no.3, pp.236-249, 2018, DOI: 10.1007/s10762-017-0453-3

[27] W. X. Tang, H. C. Zhang, H. F. Ma, W. X. Jiang, and T. J. Cui, "Concept, theory, design, and applications of spoof surface plasmon polaritons at microwave frequencies," *Adv. Opt. Mater*., vol. 7, no. 1, 1800421, August 2018, DOI: 10.1002/adom.201800421.

[28] M. Wang, H. Feng Ma, W. X. Tang, S. Sun, T. J. Cui, "Leaky-wave radiations with arbitrarily customizable polarizations based on spoof surface plasmon polaritons," *PHYSICAL REVIEW APPLIED*, vol. 12, 014036, July 2019, DOI: 10.1103/PhysRevApplied.12.014036.

[29] V. P. Shestopalov, L. N. Litvinenko, S. A. Masalov, and V. G. Sologub, "Diffraction of Waves by Arrays", Izd. Kharkov. Gos. Univ. Kharkov (1973).

[30] E. M. Khutoryan, A. I. Tsvyk "Influence of the Smith-Purcell Radiation on Electron Beam in DRO", *Telecommunications and Radio Engineering*, vol. 68, no. 3, pp. 217-229, 2009, DOI: 10.1615/TelecomRadEng.v68.i3.20.

[31] Kim K.-J., S.B. Song "Self-amplified spontaneous emission in Smith-Purcell free electron laser", *Nucl. Instr. Meth*, vol. 475, no. 1-3, pp. 158-163, December 2001, DOI: 10.1016/S0168-9002(01)01576-5

[32] A. Bakai, K. Lukin, V. Shestopalov, "Nonlinear unsteady-state theory of diffraction radiation oscillators", *Izv. Vys. Uch. Zav. Radiofizika*, vol. 22, no. 9, pp. 1117-1123, 1979.

[33] Yu. Evdokimenko, K. Lukin, I. Revin, B. Skrynnik, V. Shestopalov, "A new mechanism of excitation of a diffraction-radiation generator (free-electron laser)", *Sov. Phys. Doklady*, vol. 27, pp. 554-558, 1982.

[34] B. Goplen, L. Ludeking, D. Smith, and G. Warren, "User-configurable MAGIC for electromagnetic PIC calculations," Comput. Phys. Commun., vol. 87, no. 12, pp. 54–86, May 1995, DOI: 10.1016/0010-4655(95)00010-D

[35] A. Vertiy, I. Ivanchenko, A. Nesterenko, N. Popenko, A. Tsvyk, L. Tsvyk, v. Shestopalov, "Fine structure of millimeter-wave diffraction emission. I.", *Radiophys Quantum Electron*, vol. 28, pp. 888–894, 1985, DOI: 10.1007/BF01051846.

[36] H. L. Andrews and C. A. Brau, "Gain in the Smith–Purcell free-electron laser," *Phys. Rev. ST Accel. Beams*, vol. 7, no. 7, p. 070701, Jul. 2004, DOI: 10.1103/PhysRevSTAB.7.070701.

[37] J. T. Donahue and J. T. Gardelle, "Simulation of Smith–Purcell radiation using a particle-in-cell code," *Phys. Rev. ST Accel. Beams*, vol. 8, no. 6, p. 060702, Jun. 2005, DOI: 10.1103/PhysRevSTAB.8.060702.

[38] V. Kumar and K.-J. Kim, "Analysis of Smith–Purcell free-electron lasers," *Phys. Rev. E, Stat. Phys. Plasmas Fluids Relat. Interdiscip. Top*., vol. 73, no. 2, p. 026501, Feb. 2006, DOI: 10.1103/PhysRevE.73.026501.

[39] J. Gardelle, P. Modin, H. Bluem, R. Jackson; J. Jarvis; A. Todd, J. Donohue, "A Compact THz Source: 100/200 GHz Operation of a Cylindrical Smith–Purcell Free-Electron Laser", *IEEE Transactions on Terahertz Science and Technology*, vol. 6, no. 3, pp. 497 – 502, May 2016, DOI: 10.1109/TTHZ.2016.2543603.

[40] B. K. Skrynnik, V. K. Korneenkov, and M. Y. Demchenko, "On the feedback in the Smith–Purcell experiments,", *Telecommunications and Radio Engineering*, vol. 55, no. 10-11, pp. 55-61, 2001, DOI: 10.1615/TelecomRadEng.v55.i10-11.220.

[41] K. Lukin; E. Khutoryan; G.-S. Park, "Interaction of evanescent wave and Smith-Purcell radiation modes in resonant BWO-DRO device", 2009 *IEEE International Vacuum Electronics Conference* 28-30 April 2009, DOI: 10.1109/IVELEC.2009.5193529.

[42] V. L. Bratman, A. E. Fedotov, I. M. Khaimovich, and P. B. Makhalov, "Excitation of orotron oscillations at the double frequency of the surface wave," *Radiophys. Quantum Electron*., vol. 50, no.10-11, pp. 780–785, Oct. 2007, DOI: 10.1007/s11141-007-0068-y.

IEEE Transactions on Electron Devices, Volume 70, Issue 10, Digital Object Identifier: 10.1109/TED.2023.3301841
https://doi.org/10.1109/TED.2023.3301841